6-2022

On three-dimensional rotating viscoelastic jets in the Giesekus model

Daniel N. Riahi

Saulo Orizaga

Partial Differential Equations in Applied Mathematics 5 (2022) 100364

Contents lists available at ScienceDirect

Partial Differential Equations in Applied Mathematics

journal homepage: www.elsevier.com/locate/padiff

On three-dimensional rotating viscoelastic jets in the Giesekus model

Daniel N. Riahi [a,b], Saulo Orizaga [c,*]

[a] Department of Mechanical Science and Engineering, University of Illinois at Urbana, Champaign, Urbana, IL 61801, USA
[b] School of Mathematical & Statistical Sciences, University of Texas Rio Grande Valley, Brownsville, TX 61820, USA
[c] Department of Mathematics, New Mexico Institute of Mining and Technology, 801 Leroy Place, Socorro, NM 87801, USA

ARTICLE INFO

Keywords:
Viscoelastic jet
Rotating flows
Gravity force
Three-dimensional flows

ABSTRACT

We investigate three-dimensional nonlinear rotating viscoelastic curved jets in the presence of gravity force. Applying the Giesekus model for the viscoelastic stress parts of the jet flow system and using perturbation methods with a consistent scaling, a relatively simple system of equations with realistic three-dimensional centerlines is developed. We determine numerically the relevant solution quantities of the model in terms of the radius, speed, tensile force, stretching rate, strain rate and the jet centerline versus arc length and for different parameter values associated with gravity, viscosity, rotation, surface tension and viscoelasticity. Considering the jet flow system in full 3-dimensions and in the presence of gravity can be significant, impacting the jet speed, strain rate, tensile force, stretching rate and the centerline curvature are notably increased in magnitude and the jet radius size is reduced and this becomes more dominant with larger values of the arc length, gravity, rotation and viscoelasticity. In particular, for a typical value of the gravity and for an order one value of the arc length, we found that gravity makes jet speed higher by at least a factor of 2 and makes jet radius lower by a factor of 0.6 or smaller as we compare to the corresponding values when gravity is not considered.

1. Introduction

We are interested to study the problem of rotating jet flows with the focus on the problems in various applied areas that deal with the viscoelastic jet generation and the potential applicability in the case of fiber production technology. The governing system of partial differential equations and the boundary conditions for the jet flow system is so complex and formidable to study that only reliable modeling approach can go forward for further understanding such system and its solutions. We proceed in the present study with the development of a reliable model based on the applied mathematics methods for rather simple cases of the parameters values to determine the fundamental features of the solutions to such jet system, even though we are aware of the challenges that exist for the authors in the past whose asymptotic models for such jet system failed for the parameter values relevant to the nano-fiber jet cases, and instead a so-called regularization approach was used that drastically changed and eliminated terms in the actual partial differential equations of the fluid mechanics with no applied mathematics justification and no experimental verification (see Refs. 1, 2). However, we are very optimistic that our present applied mathematical approach based on the proper scaling and perturbation procedure, which accounts for the well-known partial differential equations of fluid flow, is the most likely one that can determine nano-fiber jet solutions and overcome such challenges in near future.

Rotationally driven flows have been extensively studied by researchers computationally, theoretically and experimentally. Such studies have been conducted considering different fluid flow conditions including inviscid, Newtonian and non-Newtonian (see Refs. 3–10) fluids. In one of the main physical characterization of the resulting jet, we find a jet of very small radius. This is in fact used in the theoretical formulation by accounting for the small aspect ratio of the jet's radius to the jet's length. Relevant theoretical and numerical investigations are reported by Decent et al.[3] in which an inviscid rotating jet in the presence of gravity and surface tension was considered. Later the same research group, Decent et al.,[5] considered a more complicated problem in 2-dimensions which modeled a Newtonian viscous jet. They reported that the viscosity in the system made the jet structure attain a high level of curvature.

In 2011, Padron et al.[6] conducted a modeling and computation investigation of a 2-dimensional inviscid rotating jet in the presence of surface tension. Their model considered is related to the forcespinning process, an experimental set up to fabricate small fibers with a rotation mechanism. The numerical solutions reported by Padron et al.[6] indicated that higher rotation rates generated thinner jets and that considering higher values of surface tension will generate contracted jet path trajectories. In order to continue to explore and understand the mechanisms of rotating flows, Padron et al.[8] conducted a follow

* Corresponding author.
E-mail addresses: d-riahi@illinois.edu (D.N. Riahi), saulo.orizaga@nmt.edu (S. Orizaga).

https://doi.org/10.1016/j.padiff.2022.100364
Received 3 November 2020; Received in revised form 17 October 2021; Accepted 27 April 2022

up experimental investigation in 2013. The experimental investigation studied the fabrication of small fiber in the forcespinning process. The use of high speed photography allowed to detect the effects of angular velocity, viscosity, jet path trajectory, jet speed and jet radius.

In 2017, Riahi[9] studied a polymeric fiber jet during the forcespinning process by implementing a phenomenological viscosity model for the polymeric non-Newtonian fluid. He simplified the rheological behavior of the polymeric fluid by considering only the viscous aspects of the extensional thinning rheology of the polymeric fluid. Similar to Wallwork et al.[4] and Decent et al.,[5] he considered a 2-dimensional model in the absence of gravity for the case of a Newtonian viscous case. He reported that the non-Newtonian fluids allowed for a more favorable thinning jet which is of particular interest in applications. More recently Riahi[10] investigated a two-dimensional rotating viscoelastic jets model in the absence of gravity. The model contained the Giesekus constitutive equations (see Ref. 11) for the stress tensor in the governing equations for the jet system. Riahi solved the proposed model for relevant quantities associated with the forcespinning process.

It should be noted that all the related two-dimensional studies in the past (see Refs. 4, 5, 9, 10) were under the restricted and unrealistic assumption that the jet centerline was in fixed horizontal plane and no effect of gravity was taken into account, which are contrary to the experimental observations (Padron et al.[8]). The importance of the present study relies in that our model now considers full three-space dimensions and the presence of gravity. Such conditions are important to construct a more realistic model since the actual experimental setting takes place in three-dimensions (see Ref. 8).

We solve our proposed model by using theoretical and numerical techniques and we obtain relevant jet flow quantities for the jet flow system such as speed, radius, strain rate, stretching rate and trajectory versus different values of the parameters that represent effects due to gravity, rotation, viscosity, surface tension, relaxation time for the polymeric extension. We find that the full three-dimension modeling of the flow along with gravity provide a destabilizing effect in the sense that values of the jet speed, stretching rate, centerline curvature and strain rate are increased and the size of the jet radius was decreased and more so with increasing the parameter values associated with gravity, rotation and relaxation time. As compared to the known results for the two-dimensional cases of polymeric jets[9,10] and Newtonian viscous jets,[5] the present three-dimensional study is able to uncover new results which show how jet fiber formation is affected by the three-dimensional realistic nature of the problem in the presence of gravity.

2. Model formulation

The modeling for the rotating viscoelastic jet considered in this paper is initially based on the original three-dimensional governing system of equations for the momentum and mass conservation[12] in a coordinate system that is placed, attached and embedded on a rotating spinneret (see Fig. 1) for a rotating system like the one for the forcespinning system.[6,8] In Fig. 1 the gravity force and the angular velocity are shown, where the axis of the angular velocity is anti-parallel to that of the gravity force, and C represents half-length of spinneret. Like the forcespinning process, the produced fibers are considered to be curved due to the rotational forces generated by the spinneret.

The following governing equations are given for the mass continuity and momentum that can represent the viscoelastic jets in the rotating frame, where in these equations the stress tensor $\mathbf{T}$ is based on the upper convected Maxwell model (Bird et al.[13]; Larson[14]):

$$\nabla \cdot \mathbf{u} = 0, \tag{2.1}$$

$$\partial \mathbf{u}/\partial t + \mathbf{u} \cdot \nabla \mathbf{u} = (-1/\rho)\nabla P + (1/\rho)\nabla \cdot \mathbf{T} - \boldsymbol{\omega} \times (\boldsymbol{\omega} \times \mathbf{r}) - 2\boldsymbol{\omega} \times \mathbf{u} + \mathbf{g}, \tag{2.2}$$

$$\mathbf{T} = \boldsymbol{\tau} + \eta_s(\nabla \mathbf{u} + \nabla \mathbf{u}^{\mathrm{T}}), \tag{2.3}$$

$$\lambda \partial \boldsymbol{\tau}/\partial t + \boldsymbol{\tau} + \lambda\{\mathbf{u} \cdot \nabla \boldsymbol{\tau} - \nabla \mathbf{u}^{\mathrm{T}} \cdot \boldsymbol{\tau} - \boldsymbol{\tau} \cdot \nabla \mathbf{u}) + \mu(\lambda/\eta_p)(\boldsymbol{\tau})^2 = \eta_p(\nabla \mathbf{u}^{\mathrm{T}} + \nabla \mathbf{u}). \tag{2.4}$$

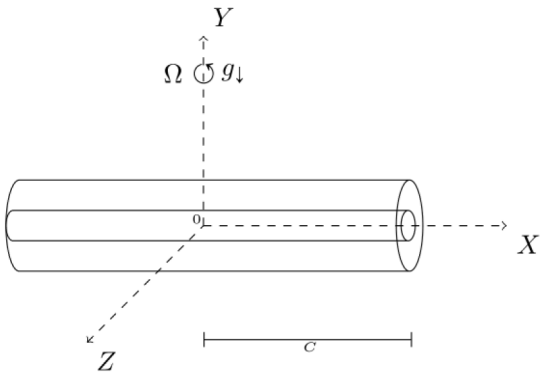

Fig. 1. Rotating spinneret and coordinate systems.

Here $\mathbf{u}$ is the relative velocity vector of the jet, P is the pressure, $\mathbf{T}$ is the stress tensor, ρ is the density of the melt or solution, $\mathbf{g}$ is the gravity force per unit mass, t is the time variable, ω is the angular velocity vector, whose magnitude is designated by Ω, of the rotating spinneret, and the orifice of the spinneret emits fiber jet from the melt or solution in the fluid container,[6,8] $\mathbf{r}$ is a position vector of a point on the jet, η_p and η_s are the viscosities of the polymer and solvent, respectively, λ is the so-called relaxation time and μ is a constant coefficient. This is a coefficient of the nonlinear stress term in (2.4) that contributes to an anisotropic hydrodynamic drag on the viscoelastic polymer flow molecules[13] whose value is in the interval [0, 1] (see Ref. 11). We also consider here a Cartesian coordinate system (X, Y, Z) that is attached to the spinneret, and we refer to it as the rotating coordinated system. Clearly, this coordinate system is fixed relative to the rotating spinneret. In contrast to the previous unrealistic and restricted two-dimensional studies,[4,9,10] we consider here a three-dimensional model that takes into account the presence of gravity force. The fiber jet's arc length condition that needs to be satisfied here in the three-dimensional space is given by

$$(\partial \mathbf{X}/\partial s)^2 + (\partial \mathbf{Y}/\partial s)^2 + (\partial \mathbf{Z}/\partial s)^2 = 1, \tag{2.5}$$

where s is the arc length along the jet's centerline. Thus, here the components of a position vector of a point on the jet's centerline with respect to the Cartesian coordinate (X, Y, Z) system are designated by $\mathbf{X}$, $\mathbf{Y}$ and $\mathbf{Z}$, respectively.

The governing equations (2.1)–(2.5) given above are needed to have relevant boundary conditions for the jet. At the free surface of the jet the relevant kinematic and dynamic boundary conditions (see Ref. 12) are given by

$$\partial \beta/\partial t + \mathbf{u} \cdot \nabla \beta = 0, \ \ \beta \equiv n - R(s, \phi, t), \tag{2.6}$$

$$(\mathbf{T} - P\mathbf{I}) \cdot \mathbf{n} = -\sigma \kappa \mathbf{n}, \tag{2.7}$$

where n is the radial variable and ϕ is the azimuthal angle representing the variables of the polar coordinate in a plane that is perpendicular to the jet centerline, $\mathbf{n}$ is a unit normal vector perpendicular to the jet's free surface boundary that points outward from the jet, $\mathbf{I}$ is a unitary matrix, R is the jet radius, σ is surface tension, and $\kappa \equiv \nabla.\mathbf{n}$ is twice mean curvature of the jet boundary. Following earlier treatment,[4,10] we presented these boundary conditions (2.6)–(2.7) in terms of independent variables of a local orthogonal curvilinear coordinates (s, n, ϕ). In addition, in the present three-dimensional jet case, the following main boundary conditions at the orifice where jet exits are needed to be satisfied

$$\mathbf{X} = \mathbf{Y} = \mathbf{Z} = \partial \mathbf{Y}/\partial s = \partial \mathbf{Z}/\partial s = 0, \partial \mathbf{X}/\partial s = 1, u = U, R = r_o \text{ at } s = 0. \tag{2.8}$$

Here U is the velocity of jet centerline at the exit section and r_o is the radius of the orifice that is located at the jet exit section.

We non-dimensionalize the governing system (2.1)–(2.7) in the earlier described orthogonal coordinate system (s, n, ϕ) by certain scaling for each variable which is as follows. We use scaling U for the velocity vector $\mathbf{u}$=(u, v, w), ρU^2 for fluid pressure, r_0 for n and R, C for s and (X, Y, Z), C/U for t and $(\eta_s + \eta_p)U/r_0$ for the stress tensor, where C is half of length of the spinneret. For simplicity of notation, we express the resulting non-dimensional variables in the non-dimensional governing system in terms of the same original symbols. The resulting non-dimensional form governing system will contain some non-dimensional parameters that are as follows. Rossby number R_b=$U/(\Omega C)$ that represents the rotational parameter, Froude number $F = U/(Cg)^{0.5}$ that represents the gravity parameter, Weber number $W_e = \rho U^2 r_o/\sigma$ that represents the surface tension parameter, Reynolds number $R_e = \rho UC/(\eta_s + \eta_p)$ that represents the viscosity parameter, Deborah number $D_e = \lambda U/C$ that represents the non-Newtonian parameter, $\eta = \eta_p/(\eta_s + \eta_p)$ that represents viscosity ratio and $\varepsilon = r_o/C$ (ε<<1) that represents a small aspect ratio parameter of the jet, where g is acceleration due to the gravity effect and λ is the relaxation time of the viscoelastic jet.

As described and used in the previous studies,[4,10] the present jet system in its non-dimensional form contains ε, which is under the reasonable condition, which is in agreement with the experimental results,[8] that the fiber jet is sufficiently long and slender, so that ε can be a very small parameter (ε<<1). Thus, in our scaling analysis that we consider here we apply the following expansions for the dependent variables:

$$(u, v, w) = [u_0(s,t) + \varepsilon n u_1(s,\phi,t) + \cdots, \varepsilon n v_1(s,\phi,t) + \cdots, \varepsilon n w_1(s,\phi,t) + \cdots], \tag{2.9}$$

$$(P, R) = [P_0(s,t) + \varepsilon n P_1(s,\phi,t) + \cdots, R_0(s,t) + \varepsilon R_1(s,\phi,t) + \cdots], \tag{2.10}$$

$$(X, Y, Z) = [X_0(s,t) + \varepsilon X_1(s,t) + \cdots, Y_0(s,t) + \varepsilon Y_1(s,t) + \cdots, Z_0(s,t) + \varepsilon Z_1(s,t) + \cdots], \tag{2.11}$$

$$\tau_{ij} = \tau_{0ij}(s)\delta_{ij} + \varepsilon n \tau_{1ij}(s,\phi) + \cdots, \tag{2.12}$$

where subscripts "ij" for τ_{ij} that we used in (2.12) indicate, respectively, normal stress components along s and n directions for $i = j = 1$ and 2, while tangential components of the stress tensor indicate the case for $i \neq j$. Also, δ_{ij} is defined to be equal to 1 if $i = j$ and 0 if $i \neq j$.

For implementation of our scaling analysis for the jet model, we use the expansions (2.9)–(2.12) in the governing system, where ε is used to scale the variables properly in the governing system. Our non-dimensional governing system is then simplified for the steady case and only the leading order terms in (2.1)–(2.5) are retained. Our additional simplifications are made to have a final system only for u_0, R_0, X_0, Y_0 and Z_0. For simplicity of notations, we drop the subscripts and the finalized and simplified form of the modeling system is then given by

$$u(\partial u/\partial s) = [1/(W_e R^2)]\partial R/\partial s - E_9/F^2 + (2u/R_b)[E_8(\partial Z/\partial s) - E_{10}(\partial X/\partial s)] + (1/R_b^2)[E_8(X+1) + E_{10}Z] + [(1-\eta)/R_e][(6/R)(\partial R/\partial s)(\partial u/\partial s) + 2(\partial^2 u/\partial s^2)] + [1/(R_e R^2)](\partial/\partial s)[R^2(\tau_{11} - \tau_{22})], \tag{2.13}$$

$$u\partial R/\partial s = -(R/2)\partial u/\partial s, \tag{2.14}$$

$$[(\partial X/\partial s)(\partial^3 X/\partial s^3) + (\partial Y/\partial s)(\partial^3 Y/\partial s^3) + (\partial Z/\partial s)(\partial^3 Z/\partial s^3)](\partial u/\partial s) + (2/3)(\partial E_0/\partial s) = 0, \tag{2.15}$$

$$[-u^2 + 1/(W_e R)]E_0 - (2u/R_b)[E_{11}(\partial Z/\partial s) - E_{13}(\partial X/\partial s)] + E_{12}/(F^2) + [1/(R_b^2)][E_{11}(X+1) - E_{13}Z] + (1/R_e)[2(\partial\eta/\partial s)(uE_0) + (7\eta E_0/3)(\partial u/\partial s) + (5\eta u/3)(\partial E_0/\partial s)] = 0, \tag{2.16}$$

$$\tau_{11} + D_e[u\partial\tau_{11}/\partial s - 2\tau_{11}\partial u/\partial s + (\mu/\eta)\tau_{11}^2] = 2\eta\partial u/\partial s, \tag{2.17}$$

$$\tau_{22} + D_e[u\partial\tau_{22}/\partial s + \tau_{22}\partial u/\partial s + (\mu/\eta)\tau_{22}^2] = -\eta\partial u/\partial s, \tag{2.18}$$

where

$$E_0 \equiv [(\partial^2 X/\partial s^2)^2 + (\partial^2 Y/\partial s^2)^2 + (\partial^2 Z/\partial s^2)^2]^{0.5}, \tag{2.19}$$

$$E_1 \equiv [(\partial Z/\partial s)(\partial^2 Y/\partial s^2) - (\partial Y/\partial s)(\partial^2 Z/\partial s^2)], \tag{2.20}$$

$$E_2 \equiv [(\partial X/\partial s)(\partial^2 Z/\partial s^2) - (\partial Z/\partial s)(\partial^2 X/\partial s^2)], \tag{2.21}$$

$$E_3 \equiv [(\partial Y/\partial s)(\partial^2 X/\partial s^2) - (\partial X/\partial s)(\partial^2 Y/\partial s^2)], \tag{2.22}$$

$$E_4 \equiv -E_2/[E_0(\partial Z/\partial s)], \tag{2.23}$$

$$E_5 \equiv E_1/[E_0(\partial Z/\partial s)], \tag{2.24}$$

$$E_6 \equiv E_1/E_0 - E_3(\partial X/\partial s)/[E_0(\partial Z/\partial s)], \tag{2.25}$$

$$E_7 \equiv E_2/E_0 - E_3(\partial Y/\partial s)/[E_0(\partial Z/\partial s)], \tag{2.26}$$

$$E_8 \equiv [E_3E_5 - E_7(\partial^2 Z/\partial s^2)]/[E_0(\partial Z/\partial s)(E_4E_7 - E_5E_6)], \tag{2.27}$$

$$E_9 \equiv [E_6(\partial^2 Z/\partial s^2) - E_3E_4]/[E_0(\partial Z/\partial s)(E_4E_7 - E_5E_6)], \tag{2.28}$$

$$E_{10} \equiv [1 - E_8(\partial X/\partial s) - E_9(\partial Y/\partial s)]/(\partial Z/\partial s), \tag{2.29}$$

$$E_{11} \equiv E_7/(E_4E_7 - E_5E_6), \tag{2.30}$$

$$E_{12} \equiv E_6/(E_4E_7 - E_5E_6), \tag{2.31}$$

$$E_{13} \equiv [E_6(\partial Y/\partial s) - E_7(\partial X/\partial s)]/[(E_4E_7 - E_5E_6)(\partial Z/\partial s)]. \tag{2.32}$$

The boundary conditions are given by

$$X = Y = Z = \partial Y/\partial s = \partial Z/\partial s = u - 1 = R - 1 = \partial X/\partial s - 1 = 0 \text{ at } s = 0, \tag{2.33}$$

$$\tau_{11} - 2\eta\partial u/\partial s = \tau_{22} + \eta\partial u/\partial s = 0 \text{ at } s = 0. \tag{2.34}$$

As noted from (2.34), for the stress conditions at the jet exit section $s = 0$ we use purely Newtonian conditions since similar to the electro-spinning case (see Ref. 15), our numerical computation indicated that our results are insensitive with respect to any changes to these stress conditions. In addition, these stress conditions at $s = 0$, turn out to be based on the result that the molecules of the viscoelastic flow have not yet been stretched at the initial location of the jet at s=0.[16]

It should be noted that from the centerline momentum equation (2.13), it can be seen that the it contains an important term due to the so-called tensile force $T_f = R^2\ (\tau_{11} - \tau_{22})$ (see Ref. 15). As is provided in the next section, the centerline rate of change of the tensile force for the fiber jet is found to be positive, and it turns out to make notable contribution to speed up the jet and, which leads to a notable reduction in the size of the jet radius.

3. Solutions and results

Before determining the numerical solutions for the jet system (2.13)–(2.32) and (2.33)–(2.34) at arbitrary arc length and presenting the corresponding results, we want to investigate first the asymptotic form of the solution to such system in the limit of very small arc length s. Such asymptotic investigation can also help to secure some additional boundary conditions that turns out to be needed in our numerical procedure, which is based on using an initial value problem, to be described below in this section. To investigate the asymptotic form of the solution to the above described system for small s, we find

$$u = 1 + a_1 s + a_2 s^2 + O(s^3), \tag{3.1}$$

$$R = 1 - 0.5a_1 s + (0.375a_1^2 - 0.5a_2) + O(s^3), \tag{3.2}$$

$$X = s + O(s^3), \tag{3.3}$$

$$Y = b_1 s^2 + O(s^3), \tag{3.4}$$

$$Z = c_1 s^2 + O(s^3), \tag{3.5}$$

$$\tau_{11} = 2\eta a_1 + d_1 s + d_2 s^2 + O(s^3), \tag{3.6}$$

$$\tau_{22} = -\eta a_1 + e_1 s + e_2 s^2 + O(s^3), \tag{3.7}$$

where the constants a_1, a_2, b_1, c_1, d_1, d_2, e_1 and e_2 satisfy the following relations

$$a_1[1+1/(2W_e)]+[(1-\eta)/R_e](3a_1^2-4a_2)=(1/R_b^2)+(3\eta/R_e)(2a_2-a_1^2), \quad (3.8)$$

$$2(1-1/W_e)+(b_1/F^2-2c_1/R_b)/(c_1^2)+[28/(3R_e)]a_1=0, \quad (3.9)$$

$$4c_1/R_b+a_1^2+2a_2+(a_2-0.25a_1^2)/W_e+4c_1/R_b + [(1-\eta)/R_e](12a_1a_2-1.5a_1^3)=(3\eta/R_e)(a_1^2-4a_1a_2)=(1/R_b)^2, \quad (3.10)$$

$$d_1-4\eta(1-\mu)a_1^2=d_2-(2a_2\eta-d_1/2)/D_e-a_1(-2\mu d_1+0.5d_1+4a_2\eta)=0, \quad (3.11)$$

$$e_1+\eta(1-\mu)a_1^2=e_2+(a_2\eta+e_1/2)/D_e+a_1(e_1-a_2\eta-\mu e_1)=0. \quad (3.12)$$

The nonlinear system (2.13)–(2.34) is solved numerically by considering it as an initial value problem with independent variable s using a finite difference scheme.[17] Due to the realization that the viscous stress terms in the system (2.13)–(2.34) contains second derivative for centerline velocity u and third derivatives for X, Y and Z, we did make use of the asymptotic solutions as are given in the system (3.1)–(3.12) at $s=0$. However, determining such asymptotic solutions requires that we know the values of three constants a_1, b_1 and c_1 in Eqs. (3.8)–(3.10). But, these three algebraic equations contain four unknown constants a_1, b_1, c_1 and a_2. Using an iterative procedure for given value of a_2, we calculated iteratively a_1 from (3.8). We then used such values for a_1 and a_2 in Eqs. (3.9)–(3.12) and found values of b_1, c_1, d_1, d_2, e_1 and e_2. Next, we did our numerical computation. This iterative procedure was carried out for several prescribed values of a_2, and we found out that the numerical values for the rate of change of the strain rate at $s=0$ is very small of order 10^{-3} and was insensitive with respect to the constant a_2, and the results for other jet quantities were also found to be insensitive with respect to the value of a_2. Hence, we carried out our actual computation by assuming $a_2=0$. We used (3.1)–(3.7) to determine the needed initial conditions for the dependent variables of our initial value problem in our numerical procedure described above.

We start by considering cases for different values of the rotational effect. Some typical effect of rotation on the jet radius are given in Fig. 2 that presents jet radius versus arc length for $W_e=1.5$, $R_e=1.0$, $F=4.0$, $D_e=1.0$, $\eta=0.1$ and three different values 1.0, 1.3 and 2.0 of the Rossby number, which is the parameter for the rotational effect. One main effect that can be observed from this figure is the destabilizing effect on the jet radius by the rotational forces since the jet radius decreases as the rotation rate increases. The same destabilizing effect by the rotational forces is also apparent in this figure as arc length increases since jet radius decreases with increasing the arc length. We also generated additional data from our numerical solutions for higher values of relaxation time, which corresponds to higher values of the Deborah number, and found similar destabilizing effect exerted by the forces due to rotation. In addition, our additional generated data indicated that the curvature of the jet trajectory increases with the rotational forces. We compared our present three-dimensional results for the jet radius with those in the two-dimensional jet case.[10] We found that as the effect of the rotational forces increases, the rotational rate of decrease of the jet radius as well as the arc length rate decrease of the jet radius in the present results were notably higher than the corresponding ones in the two-dimensional case.

We also generated data for the jet speed and the tensile force versus arc length but for the same values of the parameters as in Fig. 2. We found that again destabilizing effect of the rotational forces is apparent since both jet speed and the tensile force are enhanced with increasing the rotational forces. In addition, both jet speed and tensile.

Force increase with increasing the arc length. We also examined the present three-dimensional results for the jet speed and the tensional as we compared them with the corresponding ones in the two-dimensional jet case in the absence of the force of gravity.[10] We found that in the present realistic case of the three dimensionality nature of the jet system and the presence of the force of gravity can notably enhance at higher values the jet speed and its rate of increase with the rotation

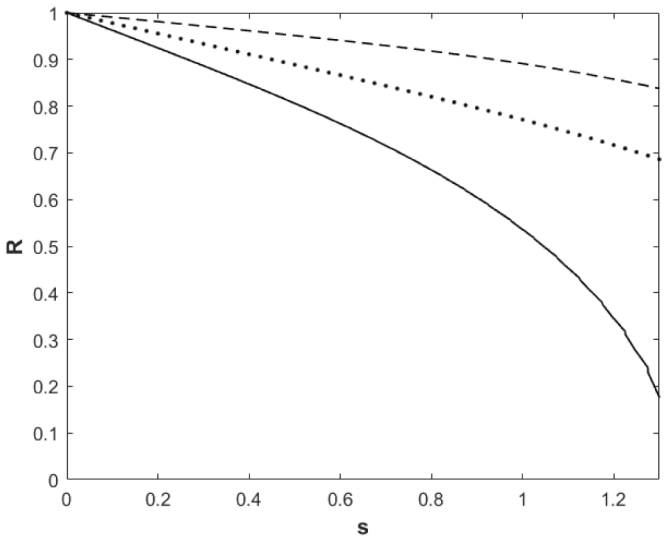

Fig. 2. Jet radius versus arc length for $W_e=1.5$, $R_e=1.0$, $D_e=1.0$, $\eta=0.1$, $F=4.0$ and three different values 1 (solid line), 1.3 (dotted line) and 2.0 (dashed line) of R_b.

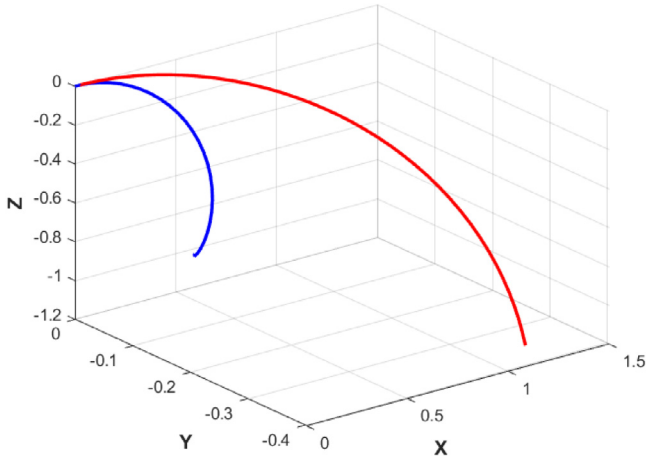

Fig. 3. Jet centerline for $R_e=1.0$, $F=4.0$, $D_e=1.0$, $n=0.9$, $W_e=1.5$, $\eta=0.1$ and for different values of $R_b=1.0$ (blue line) and 1.3 (red line).

forces or arc length than the corresponding ones in the restricted two-dimensional jet case. In the case of the tensile force, we found that the tensile force is enhanced significantly with increasing the rotation forces. In addition, we found that the tensile force and its arc length rate of change increase significantly as the arc length increases if the rotation rate is not too small.

Some typical effect of the rotational forces on the jet centerline, which is basically the jet trajectory, are shown in Fig. 3, which is drawn for the jet centerline in three-dimensional space with given values of the parameters R_e, F, D_e, η and W_e and for two values of the Rossby number. We can observe from this figure that the rotational forces have destabilizing effect on the jet centerline since both the local curvature of the trajectory curve and its tightness enhance with the rotation forces. We also determined the effect of viscoelasticity on the jet centerline by generating data from our numerical results for prescribed values of R_e, R_b, W_e, η and F and different values of the Deborah number D_e. We detected that the local curvature of the jet trajectory enhances with increasing the effect of the relaxation time.

Some typical results about the effect of the gravity force in the present three-dimensional jet case on the jet speed are provided in Fig. 4 that presents values of the jet speed versus arc length for given

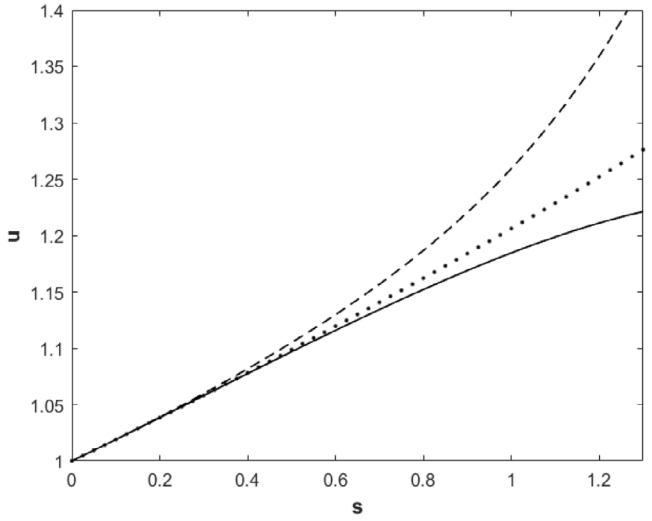

Fig. 4. u versus s for $R_e = 1.0$, $R_b = 2.0$, $W_e = 1.5$, $\eta = 0.1$, $D_e = 1.0$ and different values of $F = 4.0$ (dashed line), 10 (dotted line) and 15.0 (solid line).

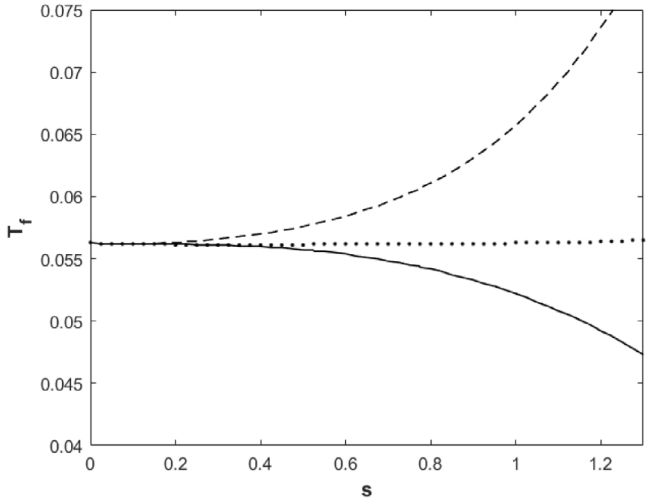

Fig. 5. The same as Fig. 4 but for tensile force versus arc length.

values of the parameters R_b, R_e, W_e, η and D_e but for three different values of the gravity parameter F. The effect of destabilization by the gravity force is apparent in this figure since the jet speed increases notably with increasing the effect of the gravity. In addition, such destabilization becomes more significant as the arc length as well as the gravity force increase. We, thus, demonstrated the significant and realistic presence of the three-dimensionality nature of the jet system and in the presence of the gravity force, that need to be taken into consideration in any jet modeling system since both three-dimensionality of the jet and the presence of gravity can have notable realistic effects in order for part of the reliability of a jet model to be developed at least in regard to the presence of such realistic effects.

We also generated data from our numerical solutions to determine some typical effect of the gravity force on the jet radius. We determined the values of the jet radius versus arc length using the values of the parameters that we chosen to be the same as those given in Fig. 4. The destabilizing effect of the gravity force on the jet radius is shown in our generated data to be significant since we found that the jet radius decreases notably as the Froude number decreases. These results by our generated data and those shown in Fig. 4 indicate that presence of gravity force and the three-dimensionality nature of the jet flow system are very important to be included in the development of a reliable model for the jet flow system, which can complement any related experimental studies that can help to design in manufacturing technologies for the production of polymeric fiber jets at micro and/or nano-scale size, which is known to have tremendous amount of applications in varies areas in science, engineering and technology.

Some typical effect of gravity force on the tensile force is provided in Fig. 5, which shows tensile force versus arc length and for the parameter values that are the same as those in Fig. 4. The results that are shown from Fig. 5 indicate that gravity force has notable destabilizing effect on the tensile force since tensile force is enhanced as the Froude number decreases. In addition, the value of the tensile force increases with the arc length, provided Froude number is not too large and the jet centerline is at some small distance away from the jet exit section

Typical results about the effects of the gravity force on the jet trajectory in the three-dimensional space are provided in Fig. 6. This figure is drawn for given parameter values R_e, R_b, W_e, η, μ and D_e and two values of the Froude number 4.0 and 10.0. In this figure the gravity force is in the direction along negative Y-axis. We can observe

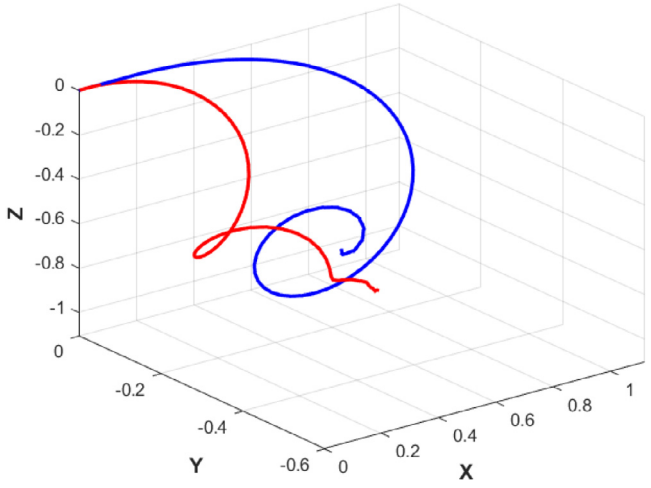

Fig. 6. Jet centerline for $R_e = 1.0$, $R_b = 2$, $W_e = 1.5$, $D_e = 1.0$, $\eta = 0.1$ and different values of $F = 4.0$ (blue line) and 10.0 (red line).

from this figure that the gravity force of gravity tends to push further the centerline of the jet in the downward direction, which causes the jet to move at higher speed in the downward direction.

To determine effect of viscoelasticity on the jet speed, we present here in Fig. 7 the graph of the jet speed versus arc length for given values of the parameters $R_b = 2.0$, $R_e = 1.0$, $F = 4$, $W_e = 1.5$, $\eta = 0.1$ and different values of the Deborah number, which is the parameter that represents viscoelasticity. The results from this figure indicate that viscoelasticity has weak destabilizing effect on the jet speed since jet speed slightly increases with the relaxation time of the non-Newtonian jet flow. In addition, the jet speed notably increases as arc length increases for some moderate distance away from the jet exit section.

To determine the effect of viscoelasticity on the jet radius, we generated numerical data for the jet radius versus arc length with given values of the parameters that are the same as the ones used to draw Fig. 7. The results of our data indicated that the values of the jet radius decrease as the value of the arc length increases in but for all those three cases for the Deborah number, and the value of the jet radius is significantly smaller a short distance away from the jet exit. The results of our generated data also indicate that at a short distance from the

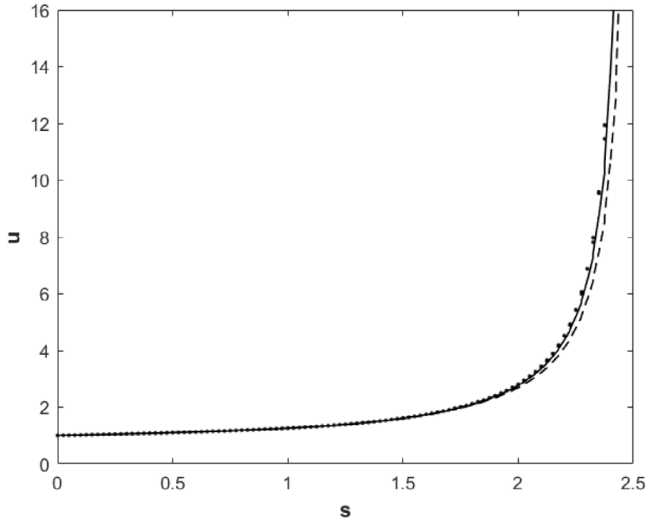

Fig. 7. u versus s for $R_e = 1.0$, $R_b = 2.0$, $F = 4.0$, $W_e = 1.5$, $\eta = 0.1$ and different cases of $D_e = 15.0$ (dotted line), 3.0 (solid line) and 1.0 (dashed line).

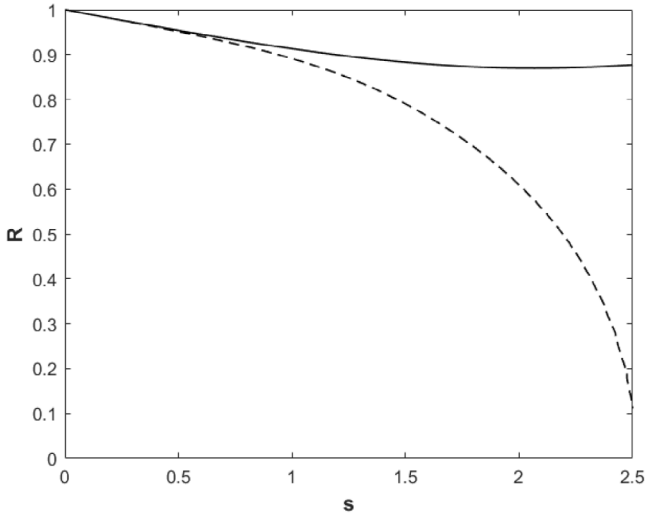

Fig. 8. Jet radius versus s for $W_e = 1.5$, $R_b = 2.0$, $R_e = 1.0$, $D_e = 1$, $\eta = 0.1$, $\mu = 0.1$ and for three-dimensional case ($F = 4.0$; dashed line) and two-dimensional case (F=∞; solid line).

jet exit, the rate of decrease of the jet radius with respect to the arc length is higher for higher value of the viscoelasticity. Our more general produced data for different values of the parameters indicated that the jet radius in the present three-dimensional model is notably smaller as compare with those results in the restricted case of two-dimensional viscoelastic jet and the case of Newtonian jet flow. It is also clear from these results that the three-dimensionality of the jet system as well the non-Newtonian viscoelastic nature of the fiber jet both are destabilizing in the present case of the non-Newtonian jet fluid flow.

Furthermore, our produced data for polymer viscosity parameter η indicated that the main effect of the polymer viscosity is to stabilize jet quantities such as the jet speed and jet radius, provided jet flow is not close to the location of the orifice. This implies that the jet speed decreases as the polymer viscosity increases, while the jet radius increases with increasing such viscosity, provided jet flow is not very close of the exit section of the jet.

To determine the effect of the force of gravity on the variations of two additional jet quantities, which are strain rate ($\partial u/\partial s$) and stretching rate ($|\partial R/\partial s|$), as the arc length increases, we generated data from our numerical solutions about these quantities versus arc length and for given values of the parameters $W_e = 1.5$, $R_b = 2.0$, $R_e = 1.0$, $D_e = 1.0$, $\eta = 0.1$ and different values of the Froude number. Our results from such data indicated that both realistic presence of three-dimensional jet and the force of gravity provide destabilizing effect on such jet quantities since both stretching rate and strain rate increase with decreasing the Froude number. In addition, these two jet quantities increase with increasing the arc length. Our additional generated data for these two jet quantities versus arc length and for different values of the Rossby number and the Deborah number indicated that the effect due to the rotation rate and viscoelasticity are also destabilizing since these jet quantities increase with increasing either the rotational forces or the viscoelastic effect.

To determine the realistic effects of the three-dimensionality nature of the jet in the presence of the gravity force, we made a direct comparison between such jet flow and the restricted case of the two-dimensional jet in the absence of the gravity by generating data for the jet radius in both of these two jet cases. Our results are presented in Fig. 8 for the jet radius versus arc length with given parameter values $R_e = 1.0$, $R_b = 2.0$, $W_e = 1.5$, $D_e = 1.0$, $\eta = 0.1$ and for the three-dimensional case ($F = 4.0$; dashed line) and the two-dimensional counterpart (F=∞; solid line). We can observe from this figure that the jet radius the three-dimensional jet flow has notably higher values than the jet radius for the two-dimensional jet, provided the jet is not too close to its exit section. Furthermore, the rate of decrease of the jet radius with respect to the arc length in the three-dimensional jet significantly higher than the one for the two-dimensional jet.

We also investigated the results based on the three-dimensional case in the presence of the gravity force, which we refer to here as the case 1, and the two-dimensional counterpart in the absence of gravity force, which we refer to here as the case 2, for several different values of the parameters. We found that for the order one values of the arc length, the jet speed in the case 1 was higher than the one in the case 2 by at least a factor of 2, and the jet radius in the case 1 was lower by a factor of 0.6 or smaller than the one in the case 2. Thus, clearly presence of gravity in the realistic three-dimensional domain makes significant differences in the results as compare to the unrealistic two-dimensional jet case.

4. Validation of present model

Our present model, which is applicable to rotating viscoelastic jet, was developed first based on the Giesekus constitutive equations[11] for the stress tensor parts of the present jet flow system and then proper scaling procedure and perturbation approaches were used to simplify the modeling system to the level that can be applicable and be valid subjected to physical and experimental conditions. So, in the following paragraphs we shall describe our motivation for selecting the Giesekus model, the physical relevance of our model and the experimental validation.

From many known constitutive models that have been developed in the past for the stress tensor of the governing non-Newtonian fluid flow system,[18] we just similar to many other authors in the past in the area of viscoelastic fluid cases, implemented the Giesekus model that has been used in the past studies by many investigators in their non-Newtonian fluid flow studies such as in the investigated work for the electrically driven viscoelastic jet.[15] In contrast to a number of models that have been developed for the constitutive equations of the stress tensor parts of the governing partial differential equations for the viscoelastic fluid flow[18] that lack important nonlinear stress terms in their developed constitutive equations, the Giesekus constitutive equations contain important nonlinear stress terms. In addition, the

Giesekus model is known to be able to detect a number of realistic features of the real viscoelastic fluid flow and its nonlinear rheological properties in the experiments and in the technological applications. Also, in forcespinning process to produce fiber with applications in fine fiber production technology that present results for the viscoelastic jets can be relevant, it is known[8] that large deformations take place in a short period in time and the nonlinear polymeric models such as the Giesekus model are suggested to be used in theoretical and computational studies of the rotating viscoelastic fiber jet system[8]. Thus, in the present study we have used such model in order to be able to detect more realistic features of the rotating viscoelastic fiber jet quantities.

Our model is then developed by following the slender jet theory, which is consistent with the observation in the related experiments and is relevant in the corresponding applications in technology. Such theory then introduces a very small parameter, which is the aspect ratio for the jet, and we made use of such parameter as the one for our perturbation procedure and expansion under proper scaling that is fully in agreement with the physical laws that various quantities such as fluid viscosity, surface tension, polymer viscosity, rotation and viscoelasticity can obey and vary. As a result of such developed model the solutions for the quantities of the jet flow system such as jet speed, radius, tensile force, strain rate, jet trajectory and stretching rate all were found to follow physical meaningful results, which were described in detail in the last section, and, thus, such physically meaningful results further add to the validation of our model.

Additional validation of our model was found by direct comparison of our results with those observed in the relevant experiments (see Ref. 8). These authors in this reference studied experimentally production of fiber jets that can made during the forcespinning process. High speed photography was used in order to understand the way fiber is produced through the forcespinning process. As a result of their experimental studies, they collected data and were able to determine some fiber jet quantities and their effects for different values of angular velocity of the rotating spinneret and the polymer viscosity of the viscoelastic fluid solution. Their selected fluid solution was a weight percentage of PEO (Polyethylene oxide) concentration in water. The jet quantities that these authors were determined include those such as jet trajectory, jet speed and jet radius. Their results on the way such quantities vary with respect to certain parameters that they were able to control and vary such as angular velocity of rotation and polymer viscosity were found to agree completely and qualitatively with the present results. Of course, it was not expected to have quantitative agreement between the present results and those in their experiments due to different parameter values that were used there as well as other effects that were presented in the experiments that were not included in the present model such as presence of fiber collection system, evaporation of the solvent, aerodynamic force and temperature effects.

5. Conclusion

Three-dimensional nonlinear system of partial differential equations for the rotating viscoelastic jet system in the presence of force of gravity were simplified by using proper scaling and perturbation techniques in the Giesekus modeling formulation. We determined the solutions to this simple system both asymptotically and by numerical computation. We uncovered effects due to the realistic three-dimensionality of the jet system in the presence of the force of gravity on the jet quantities for different values of the rotational forces, viscoelasticity of the polymeric fluid flow, gravity force and the polymeric viscosity.

We highlight here the main findings that are given below:

(i) The values of the three jet quantities speed, stretching rate and the strain rate were increased notably by the three-dimensionality nature of the jet and by increasing the strength of the force of gravity.

(ii) The values of the above three jet quantities increased as the arc length of the jet centerline increased from a very short distance from the orifice, and the values of these quantities increased with increasing the effects due to viscoelasticity and the rotational forces and decreased with increasing the polymeric viscosity

(iii) The value of the jet radius decreased notably by the three-dimensionality of the jet centerline and by increasing the strength of the force of gravity, but the value of the jet radius increased with the polymeric viscosity.

(iv) The value of the jet radius decreased as the values of the arc length of the jet centerline, rotational forces and the viscoelastic effect increased with increasing the effects due to the rotation and the viscoelastic effect.

(v) For order one values of the arc length and for various values of the parameters, presence of gravity force made jet speed higher by at least a factor of 2 and made jet radius lower by a factor of 0.6 or smaller as compare to the corresponding values in the absence of gravity case.

(vi) We detected that certain effects were destabilizing the jet flow since increasing such effects increased both the strength of the jet flow and the curvature of the jet centerline. These effects were found to be due to three-dimensional structure of the jet flow, rotational forces, viscoelastic effect of the polymeric flow and the presence of the force of gravity force.

(vii) We also determined that the effects due to surface tension and the polymeric viscosity are stabilizing since they reduce strength of the jet flow.

Declaration of competing interest

The authors declare that they have no known competing financial interests or personal relationships that could have appeared to influence the work reported in this paper.

Acknowledgments

S.O would like to thank Cristina Villalobos, Timothy Huber and Elda Leal for the office space and hospitality at the University of Texas Rio Grande Valley (UTRGV) during the summer of 2021. S.O also thanks Anwar and Elizabeth from NMT for their continued support.

Appendix

Nomenclature of symbols

c	half-length of spinneret
F	Froude number
$\mathbf{I}$	unitary matrix
n	unit normal vector
R	jet radius
R_b	Rossby number
r	position vector
$\mathbf{T}$	stress tensor
$\mathbf{u}$	jet velocity vector
U	centerline velocity at jet exit
w	velocity in azimuthal direction
(X, Y, Z)	Cartesian coordinate system
$\mathbf{Y}$	Y-coordinate of a point
β	n–R
λ	relaxation time
η_p	polymer viscosity
μ	drag coefficient
Ω	magnitude of $\boldsymbol{\omega}$
ϕ	azimuthal angle

σ	surface tension
τ_{11}	normal stress along s
τ_{22}	normal stress along n
D_e	Deborah number
g	acceleration due to gravity
n	radial variable
P	pressure
r_0	orifice radius
R_e	Reynolds number
s	arc length
T_f	tensile force
u	centerline velocity
v	radial velocity
W_e	Weber number
$\mathbf{X}$	X-coordinate of a point
$\mathbf{Z}$	Z-coordinate of a point
∇	gradient vector
η	viscosity ratio
η_s	solvent viscosity
$\boldsymbol{\omega}$	angular velocity vector
ε	aspect ratio parameter
ρ	fluid density
$\boldsymbol{\kappa}$	twice mean curvature
$\boldsymbol{\tau}$	stress tensor–solvent viscous term

References

1. Taghavi SM, Larson RG. Regularized thin-fiber model for nanofiber formation by centrifugal spinning. *Phys Rev E*. 2014;89:023011.
2. Taghavi SM, Larson RG. Erratum: Regularized thin-fiber model for nanofiber formation by centrifugal spinning. *Phys Rev E*. 2014;89:059903, (E).
3. Decent SP, King AC, Wallwork IM. Free jets spun from a prilling tower. *J Eng Math*. 2002;42:265–282.
4. Wallwork IM, Decent SP, King AC, Schulkes RMSM. The trajectory and stability of a spiraling liquid jet: Part I. *Inviscid Theory J Fluid Mech*. 2002;459:43–65.
5. Decent SP, King AC, Simmons MJH, Parau EI, et al. The trajectory and stability of spiraling liquid jet: Viscous theory. *Appl Math Model*. 2009;33:4283–4302.
6. Padron S, Caruntu ID, Lozano K. On 2D forcespinning modeling. In: *Proceedings of the 2011 ASME International Mechanical Engineering Congress and Exposition, IMECE2011-64823, 7, 821-830, November (2011) 11-17, Denver, Colorado, USA*. 2011.
7. Altecor A, Mao Y, Lozano K. Large-scale synthesis of tin-doped indium oxide nanofibers using water as solvent. *Funct Mater Lett*. 2012;5(1):1250020, 4.
8. Padron S, Fuentes A, Lozano K. Experimental study of nanofiber production through forcespinning. *J Appl Phys*. 2013;113(2):024318.
9. Riahi DN. Modeling and computation of nonlinear rotating polymeric fiber jets during forcespinning. *Int J Nonlinear Mech*. 2017;92:1–7.
10. Riahi DN. Nonlinear rotating viscoelastic jets during forcespinning process. In: *Proceeding of the Royal Society of London, Series A, Vol. 474*. 2018:20180346.
11. Giesekus H. A simple constitutive equation for polymer fluids based on the concept of configuration-dependent tensorial mobility. *J Non-Newton Fluid Mech*. 1982;11:69–109.
12. Chahhahra RP, Richardson JF. *Non-Newtonian Flow and Applied Rheology*. second ed. Oxford, U.K: Butterworth-Heinemann; 2008.
13. Bird RB, Curtiss CF, Armstrong RC, Hassager O. *Dynamics of Polymeric Liquids, 1, Fluid Mechanics*. New York: Wiley; 1987.
14. Larson RG. *The Structure and Rheology of Complex Fluids*. Oxford; 1998.
15. Feng JJ. Stretching of a straight electrically charged viscoelastic jet. *J Non-Newton Fluid Mech*. 2003;116:55–70.
16. Carroll CP, Joo YL. Electrospinning of viscoelastic Boger fluids: Modeling and experiments. *Phys Fluids*. 2006;18:053102.
17. Ascher UM, Mathheij RMM, Russell RD. *Numerical Solution of Boundary Value Problems for Ordinary Differential Equations*. Philadelphia, PA, USA: SIAM Publication; 1995.
18. Zhou H, Kang W, Krener A, Wang H. Observability of viscoelastic fluids. *J Non-Newton Fluid Mech*. 2010;163:425–434.